Nanofluids Based on Pd Nanoparticles and a Linear Silicone-Based Fluid: Toward Highly Efficient Heat Transfer Fluids for Concentrated Solar Power

Desireé de los Santos, Juan Jesús Gallardo, Iván Carrillo-Berdugo, Rodrigo Alcántara, Patrice Estellé, Saray Gragera, María Gragera, Javier Navas

Nanofluids based on Pd nanoparticles and a linear silicone-based fluid: towards highly efficient heat transfer fluids for concentrated solar power

Desireé De los Santos†, Juan Jesús Gallardo†, Iván Carrillo-Berdugo†, Rodrigo Alcántara†, Patrice Estellé‡, Saray Gragera†, María Gragera†, Javier Navas†,*

†Affiliation 1: Department of Physical Chemistry, University of Cádiz, E-11510 Puerto Real, Spain.

‡ Affiliation 2: Univ Rennes, LGCGM, F-35000 Rennes, France.

Corresponding Author:

*Javier Navas (javier.navas@uca.es).

Abstract

Meeting the growing energy demand with the lowest environmental impact is one of the greatest challenges facing our society. To this end, improving the efficiency of solar energy technologies is a must. In this work, nanofluids based on a linear silicone-based fluid and Pd nanoparticles were prepared. The linear silicone-based fluid has been designed for use in concentrating solar power involving parabolic trough collector technology (CSP-PTC). The nanofluids showed high physical and chemical stability. In addition, the Pd-based nanofluids showed enhanced isobaric specific heat and thermal conductivity values without a significant increase in viscosity. The increase of the specific heat with respect to the base fluid was about 5.5%, while thermal conductivity increased by 8.5%. Analysing the interactions between the nanoparticles and the base fluid provides a clearer understanding of the improvements in these properties. Finally, the properties measured were used to analyse the performance of the nanofluids in CSP-PTC, considering the collector and the exchanger efficiency. The overall efficiency improved by about 50%, which is a promising result.

Keywords: Nanofluids; Concentrated solar power; Thermal properties; Rheological properties; Parabolic trough collectors.

Nomenclature

C_P	Isobaric specific heat ($J \cdot Kg^{-1} \cdot ºC^{-1}$)
k	Thermal conductivity ($W \cdot m^{-1} \cdot ºC^{-1}$)
L	PTC array total length (m)
$\dot{q}$	Heat transfer rate ($J \cdot s^{-1}$)
T	Temperature (ºC)
$\dot{V}$	Volumetric flux ($m^3 \cdot s^{-1}$)

Greek symbols

ρ	Density ($kg\ m^{-3}$)
ψ	Efficiency (-)
ṽ	Flow rate ($l \cdot s^{-1}$)
γ	Surface tension ($N \cdot m$)

Subs and superscripts

bf	Base fluid
coll	Collector
hex	Heat exchanger
nf	Nanofluid
out	Outlet
sys	Overall CSP-PTC system

Abbreviations

BP	Biphenyl
CSP	Concentrating Solar Power
DFT	Density Functional Theory
DLS	Dynamic Light Scattering
DPO	Diphenyl Oxide
DSC	Differential Scanning Calorimetry
GGA	Generalized Gradient Approximations
HDMS	Hexamethylsiloxane
HTF	Heat Transfer Fluid
MXene	Ti_3C_2
NTU	Number of transfer units
ODT	1-octadecanethiol
PAW	Projector Augmented Wave
PBE	Perdew–Burke-Ernzerhof
PDMS	Polydimethylsiloxane
PTC	Parabolic Trough Collector
TCE	Thermal Conductivity Enhancement
THB	Transient Hot Bridge
UV-Vis spectroscopy	Ultraviolet-visible spectroscopy
VASP	Vienna Ab-initio Software Package

1. Introduction

Among the main challenges facing our society is to meet the enormous demand for energy while creating the lowest environmental impact [1, 2]. To this end, improvements in the efficiency of the most environmentally-friendly energy sources are necessary and are the subject of a great deal of research. Among these energies, solar energy is the most promising, with concentrated solar power (CSP) being one of the technologies of greatest interest in recent times [3]. In this energy source, solar radiation is concentrated on a heat transfer fluid (HTF) that is capable of storing and transporting thermal energy to a heat exchanger to generate steam that produces electricity in a turbine. The properties of the heat transfer fluid used is one of the factors influencing the efficiency of the plants. One of the CSP technologies is based on parabolic trough mirrors (CSP-PTC), in which the fluid typically used is a thermal oil, specifically the eutectic mixture of biphenyl (BP) and diphenyl oxide (DPO). This is not an environmentally friendly fluid, showing a certain degree of toxicity. Thus, new fluids have emerged to replace this thermal oil, one of the most interesting being siloxane-based fluids, known as linear silicone fluids. These fluids are dimethylsiloxane polymers and are generally called polydimethylsiloxane (PDMS). Their properties depend on the number of monomers in their composition, and therefore they have diverse applications. Specifically, for CSP-PTC, these fluids are environmentally friendly, less toxic and less irritating. While this linear silicone-based fluid shows similar thermal conductivity and viscosity values to the eutectic mixture of biphenyl and diphenyl oxide, it has an interesting property, namely that it is capable of working at 425ºC, while the conventional fluid works up to 400ºC. However, some of its properties, such as specific heat and density, are slightly worse than those of the conventional fluid, a drawback that must be overcome. Research is required to enhance the properties of these fluids to improve the overall efficiency of CSP-PTC plants. One

interesting strategy is the development of nanofluids based on PDMS. Nanofluids are colloidal suspensions of nanoparticles in a base fluid. When these suspensions are physically and chemically stable, they usually present improved thermal properties relative to the base fluid [4]. Many studies have been conducted using nanofluids based on different nanomaterials, mainly metals [5] and metal oxides [6]. Various fluids have also been tested, the main ones being water [7] and ethylene glycol [8]. For CSP-PTC, nanofluids have been developed using conventional fluid-based eutectic mixture, employing metals [9], metal oxides [10], or transition metal chalcogenides [11]. However, nanofluids based on linear silicone-based fluid have not been widely studied as this fluid is new for CSP applications. Some research has studied nanofluids based on similar fluids. For example, Wan et al. reported nanofluids based on dimethyl silicone oil and carbon nanotubes, which showed a photothermal conversion efficiency above 50%, and a good stability under a irradiation of 19 Sun [12]. Also, nanofluids based on MXene (Ti_3C_2) and a silicone oil were reported with an increase of about 64% in thermal conductivity while the viscosity does not change with the addition of MXene into silicone oil [13].

In this work, we report the preparation and characterization of nanofluids based on a linear silicone-based fluid named Helisol 5A©, supplied by Wacker™, which has been designed to be applied in CSP-PTC plants. Pd nanoparticles were the nanomaterial used. Pd nanoparticles were chosen because of the high values of thermal conductivity. In addition, previous studies have shown good results for Pd-based nanofluids using other base fluid, that is eutectic mixture of biphenyl and diphenyl oxide. Enhancements of about 11% and 17% in thermal conductivity and heat capacity were reported for a Pd concentration of 0.06 wt.% at about 100ºC [14, 15]. The nanofluids prepared were widely characterized, their physical stability was studied, and measurements were taken of the properties of interest for heat transfer

applications, namely surface tension, density, viscosity, isobaric specific heat and thermal conductivity. Moreover, an analysis was conducted of the performance of the nanofluids in CSP-PTC plants. Finally, by theoretical calculations, the interactions between the fluid and the nanomaterial were analysed to understand the improvements in the thermal properties of the nanofluids.

2. Materials and methods

2.1. Nanofluids preparation

In this work, the nanofluids prepared were based on Pd nanoparticles (Pd nanopowder, size <25 nm, purity ≥99.5%, supplied by Sigma-Aldrich), with a commercial linear silicone-based fluid as the base fluid. This fluid is based on polydimethylsiloxane (PDMS, commercially named as Helisol 5A, supplied by Wacker, dynamic viscosity 4-6 mPa·s at 25ºC). First, a solution of a surfactant, 1-octadecanethiol (ODT, purity ≥98.0%, density 0.847 $g \cdot cm^{-3}$, supplied by Sigma-Aldrich), was prepared as the host fluid. This was achieved by adding 1 wt.% of ODT to 100mL of PDMS. Next, 0.01 wt.% of Pd nanoparticles were added to the host fluid to prepare an initial nanofluid. The mixture was sonicated using an ultrasound probe (model GM4200, supplied by Bandelin Electronics©) at 50% amplitude for 4 h with a 2:4 seconds on:off pulsation in a thermostatic bath at 20 ºC to prevent overheating. Then, aliquots were taken from the stock nanofluid to prepare nanofluids with mass fractions of Pd nanoparticles equal to $0.5 \cdot 10^{-3}$ wt.%, $1 \cdot 10^{-3}$ wt.% and $2 \cdot 10^{-3}$ wt.% by the addition of the host fluid up to 50 ml. The dilutions were sonicated for 5 min at 50Hz using an Elmasonic Select 30 bath.

2.2. Nanofluids characterization

Since ensuring that nanofluids are highly stable is a key issue for heat transfer applications, the stability of the nanofluids prepared was analysed. UV-Vis spectroscopy was used to determine the extinction coefficient, which provides information about the heat carriers in the fluid. The extinction coefficient values were obtained using a UV-Vis system assembled in our laboratory comprising a DH-2000-BAL light source and USB2000+ general purpose spectrometer, both supplied by OceanOptics. The extinction coefficient values were recorded at 500 nm, three times per day for 24 days. Particle size measurements were also performed using the dynamic light scattering (DLS) technique to analyse the physical stability of the nanofluids. This method is able to determine the solvodynamic diameter of the nanoparticles in suspension. The values were obtained using a Zetasizer Nano ZS supplied by Malvern Instruments. Particle sizes were measured for 24 days, performing measurements three times per day.

The performance of the nanofluids in heat transfer applications is related to several properties, namely surface tension, density, dynamic viscosity, isobaric specific heat and thermal conductivity. Thus, these five properties were measured to characterize the nanofluids after they reached the physical stability. These properties were then used to study the application of nanofluids in CSP-PTC plants. The pendant drop method was used to measure the surface tension, using OCA25 device supplied by Dataphysics. The dosage volume was 5 μL with a dosage rate of 0.1 μL·s-1, using a Hamilton 250 μL syringe. Ten measurements were performed for each nanofluid at 25 ºC. Density was measured using the excitation pulse technique (DM densitometer, Anton Paar) at 25 ºC. Five measurements were performed for each nanofluid at room temperature. Moreover, the dynamic viscosity in a

temperature range between 25 ºC and 175 ºC was measured under steady-state condition using a concentric cylinder geometry (Bob diameter: 27.99 mm; Bob length: 41.99 mm; Cup diameter: 30.36 mm) and the shear rate ranged between 1 s^{-1} and 100 s^{-1}, using a HR10 viscometer supplied by TA Instruments. Finally, thermal properties, namely isobaric specific heat and thermal conductivity, were measured because they are most relevant properties for heat transfer applications. Isobaric specific heat was measured using the temperature modulated differential scanning calorimetry technique. A DSC 214 Polyma calorimeter supplied by Netzsch was used. The temperature program used can be summarized as: first, temperature was set to 100 ºC for 10 min to remove contaminants before the samples were equilibrated at 20ºC for 10 min. For these two steps, the ramp rate was 10 °C·min^{-1}. Next, a temperature-modulated dynamic step was performed from 20 to 205 °C at 1°C·min^{-1} with a modulation of ±1 °C in amplitude and 120 s in periodicity. This step is included to determine the isobaric specific heat. Finally, the cooling rate was 1ºC·min^{-1}. Thermal conductivity was measured at different temperatures (from 25 to 100ºC) by means of the transient hot bridge (THB) method, using a hot point sensor connected to a THB-100 system supplied by Linseis. To reduce the natural convection during the measurements, a dry block heater, model DB 5.2, supplied by IKA was used. This system was set between room temperature and 110 ºC to measure the thermal conductivity. An input power of 30 mW was established to obtain a good signal-to-noise ratio. Ten replicas were performed for each measurement, using a measurement time of 20 s and a delay time between the replicas of 30 s to equilibrate the temperature.

2.3. DFT simulations of Pd-PDMS interfaces

We employed the VASP code [16-19] for a DFT study of the adsorption of hexamethyldisiloxane (HMDS) on Pd (111), (100), and (110) surfaces. HMDS is taken as a simplified representation of PDMS, with analogous chemistry but a less complex conformational profile, which eases convergence during optimisation without compromising the purpose of the study. Surfaces are represented by supercells in which the relevant surface terminations are limited by a vacuum slab of a thickness equal to 20 Å that minimises unphysical interactions between periodic images along its normal direction. The HMDS is initially placed so that each Si atom is located at one of the high symmetry sites on the surface terminations, and then subjected to structural relaxation. In these calculations, we used the GGA-PBE functional [20] with Grimme's D3 dispersion corrections [21, 22] to correctly describe van der Waals interactions. Valence wavefunctions were described by sets of planewaves with kinetic energies up to 400 eV, and interactions between valence electrons and ionic cores were described using PAW pseudopotentials [23, 24]. The Brillouin zone was sampled using a Monkhorst-Pack 3x3x1 k-point mesh [25, 26]. A Methfessel-Paxton smearing of 0.2 eV was used to describe orbital occupancies [27]. Dipole moment corrections were applied to the total energy. The ionic relaxation is performed under the conjugate-gradient algorithm, which iterates until the norms of all the forces in the supercell are smaller than 0.01 $eV \cdot Å^{-1}$.

3. Results and discussion

3.1. Nanofluid stability

The stability of the nanofluids is one of the main issues affecting their performance in heat transfer applications. Thus, the physical stability of Pd-based nanofluids was analysed by means of extinction coefficient and particle size measurements. The extinction coefficient was estimated from UV-Vis spectra in which the absorption and scattering of the incident light is observed. These measurements give an idea of the load of heat carriers dispersed in the fluid. Figure 1a shows the extinction coefficient values recorded at 500 nm for the three nanofluids prepared, measured for the 24 days after the nanofluids were prepared. According to the initial values, the higher the Pd concentration, the higher the extinction coefficient values, as expected. All the nanofluids underwent aggregation during several days after their preparation, evidenced by the decrease in the extinction coefficient values during the first few days. After this period, the values remained practically constant, with only minor changes observed, which means the nanofluids reached equilibrium. In addition, the nanofluid with lowest initial concentration of Pd presented the lowest extinction coefficient values, which means the load of heat carriers was small, and therefore it would not be expected to present promising thermal properties. The extinction coefficient values for the other two nanofluids were significantly higher, suggesting that they are the most promising. On the other hand, Figure 1b shows the particle size distribution recorded for the three nanofluids from dynamic light scattering measurements for 24 days. In the case of the nanofluids with the lowest concentration of Pd, the particle size values increased during the first few days after preparation, which is the aggregation period described previously. Afterwards, the values decreased dramatically, values close to zero being obtained. This is due to the low presence of Pd nanoparticles in suspension in the fluid, as discussed above

from the extinction coefficient values. For the other two nanofluids, we observe again an increase in the particle size values during the first few days after preparation, that is the aggregation period, after which the values decrease to several hundred nanometres. The values then remained practically constant, which means the nanofluids reached the stability. This is coherent with the results shown from the extinction coefficient measurements.

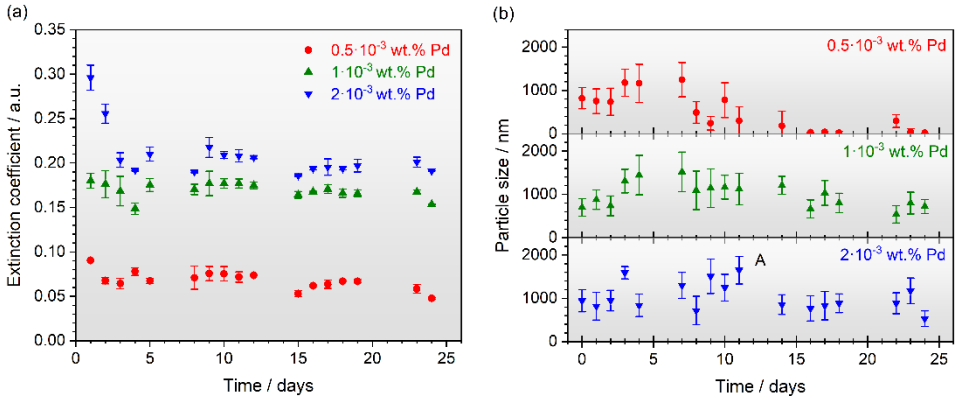

Figure 1. (a) Extinction coefficient, and (b) particle size values registered for the three Pd-based nanofluids prepared.

3.2. Nanofluid properties

The performance of nanofluids in heat transfer applications can be analysed by evaluating the heat transfer coefficient, which depends on several properties, such as surface tension, density, viscosity, isobaric specific heat and thermal conductivity. These properties were characterized to evaluate the performance of the Pd-based nanofluids prepared. The linear silicone-based fluid used as the base fluid was also characterized for comparison purposes. The mixture of the fluid and the surfactant, named the host fluid, was also characterized to analyse the effect of the surfactant on the nanofluid systems.

The surface tension values are shown in Figure 2a. The value obtained for the base fluid was 18.97 mN m^{-1}. Since the supplier does not provide the surface tension for the base fluid in the product datasheet, our value cannot be compared. The changes in the surface tension values of the nanofluids with regard to the base and host fluids are very slight, 0.02% the highest increase found for the most concentrated nanofluid. This percentage is really insignificant.

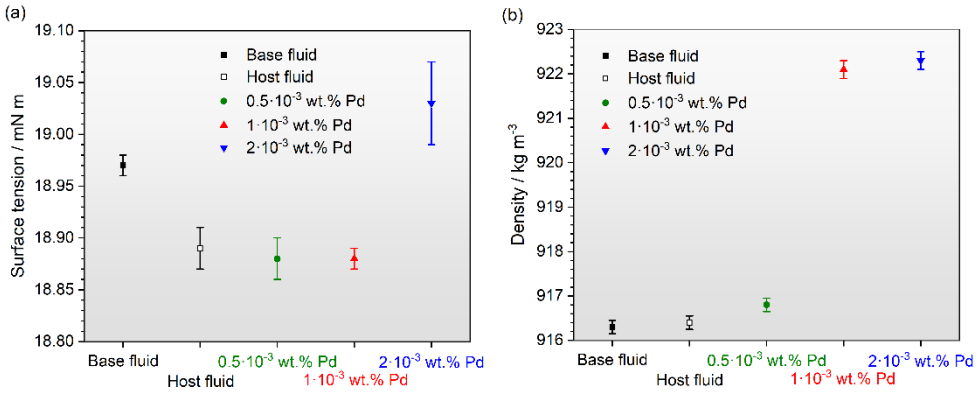

Figure 2. (a) Surface tension, and (b) density values measured of the nanofluids prepared, and the base and hosts fluids at 25ºC.

As an increase in the density values is known to enhance the heat transfer process, the density of the nanofluids and the base and host fluids was measured. Figure 2b shows the values obtained. The value obtained for the base fluid was 916.3 kg m^{-3}, close to the value of 920 kg m^{-3} provided by the supplier [28], which means a deviation of 0.4%. In addition, the density values for the host fluid and for the nanofluid with the lowest concentration of Pd nanoparticles are very similar to that for the base fluid, increases in density about 0.01% and 0.05% being obtained, values within the deviation of the measurements. This low increase in density in these cases is due to the low concentration of surfactant used to prepare the host

fluid and, in the case of the nanofluid with the lowest concentration, due to this low concentration and to the aggregation and sedimentation processes shown previously from the extinction measurements. Those results showed a very low concentration of Pd nanoparticles when the equilibrium was reached, as is discussed previously, and they are coherent with the density values obtained. The values for the two more concentrated nanofluids are clearly higher, density increases of about 0.63% and 0.65% found for the nanofluids with 1.0 wt.% and 2.0 wt.% of Pd nanoparticles, respectively. These results are in good agreement with those shown from the extinction measurements, in which a higher load of heat carriers was found for the two more concentrated nanofluids.

Viscosity is one of the most important properties for heat transfer fluids. High viscosity values are counterproductive in heat transfer processes because more pumping power is required. In the case of nanofluids, an increase in their viscosity compared to the base fluid is expected and is something that must be controlled. Thus, dynamic viscosity was measured in the 25-175 ºC range. The nanofluids, base fluid and host fluid were characterized in this range, and the shear flow plots are shown in Figure 3a-e. According to Figure 3a, for the shear rate and the temperature ranges studied, the dynamic viscosity of the base fluid is mainly constant with the shear rate, which means it shows a Newtonian behaviour. The behaviour of the host fluid and the three nanofluids prepared is similar, which means the addition of the surfactant and the Pd nanoparticles does not change the rheological behaviour of the base fluid. From the shear flow plots, the values of the dynamic viscosity can be extracted. Figure 3f shows the values of the dynamic viscosity with respect to the temperature for all the systems analyzed. The value of the dynamic viscosity of the base fluid obtained at 25 ºC was 4.73 mPa·s, which is in the range given by the supplier (4-6 mPa·s) [28]. The evolution of the dynamic viscosity values with temperature is expected; that is, the higher

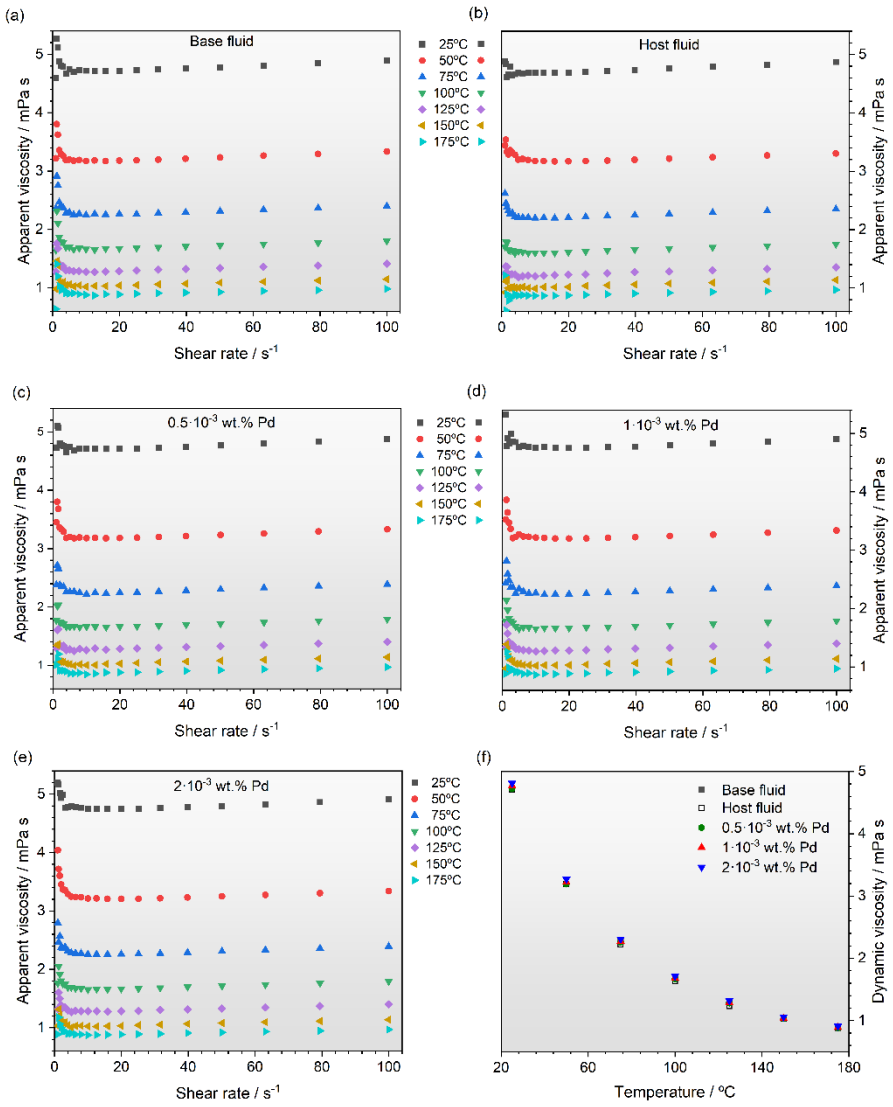

Figure 3. Shear flow plots of (a) the base fluid, (b) the host fluid, the mixture of the base fluid and the surfactant, and the nanofluids with the Pd concentration of (c) $0.5 \cdot 10^{-3}$ wt.%, (d) $1.0 \cdot 10^{-3}$ wt.%, and (e) $2.0 \cdot 10^{-3}$ wt.%. (f) Values of the dynamic viscosity vs temperature obtained from the shear flow plots.

the temperature, the lower the viscosity values. According to Figure 3f, the values obtained for the nanofluids do not increase significantly. The highest increase is observed for the most concentrated nanofluids was about 2.5%, which is similar to increases in viscosity for Pd

nanofluids using the eutectic mixture of DPO and BP as the base fluid reported previously (3.7% at 25ºC [15]). This is an interesting result because the presence of Pd nanoparticles in our nanofluids does not lead to a significant increase in the viscosity values, and also the nanofluids maintain the Newtonian behaviour of the base fluid. Therefore, the use of these nanofluids should not result in a significant increase in the pumping power needed, or in the friction factor and pressure drops.

Isobaric specific heat was also measured to analyse the heat storage capacity of the nanofluids prepared in comparison with the base fluid. Figure 4a shows the values obtained for the nanofluids, the base fluid and the host fluid. According to the values given by the supplier [28], we verify a good agreement between the values measured and those from the reference database, with a mismatch of 1.0% in the temperature range studied. The relative standard deviation is shown in the Figure 4a and is always better than 2%. We observe an increase in the isobaric specific heat with temperature, as expected. Moreover, the addition of ODT as the surfactant does not lead to significant changes in the C_P values. The nanofluid with the lowest concentration of Pd nanoparticles shows values similar to those measured for the base fluid. Only a small decrease of about 1.8% is observed when the temperature increases. This result is coherent with previous results showing that the load of heat carriers in the system after stabilisation is very low. The nanofluids with nominal Pd nanoparticle concentrations of $1.0 \cdot 10^{-3}$ and $2.0 \cdot 10^{-3}$ wt.% do not show significant differences between them due to a similar presence of Pd nanoparticles after stabilisation, as is shown above. However, the most important result is that both of these nanofluids show values higher than the base fluid, the highest increase being about 5.5%. This value is lower compared with other Pd-based nanofluids, for example using the eutectic mixture of diphenyl oxide and biphenyl as the base fluid. Those nanofluids showed an increase of 17% in isobaric specific heat [14]. But the

increase in this property is explained in new studies from the strength of the interactions between the fluid molecules and the nanomaterial, and these interactions obviously depend on the nature of the fluid. Typically, the isobaric specific heat for solids is lower than for liquids; thus, from mixture law, a decrease in the isobaric specific heat in nanofluids is expected [29, 30]. However, some studies in the literature report the opposite behaviour [14, 31]. Among the researchers that have discussed this increase, Shin et al. [32, 33] suggested this increase in isobaric specific heat is due to the formation of a certain internal structure in nanofluids due to the interaction between nanoparticles and the base fluid. Carrillo-Berdugo et al. [14] presented evidence of the formation of a strong interfacial layering effect in nanofluids based on metal nanoparticles, which affects the specific heat values.

The increase in isobaric specific heat found is an interesting result for heat transfer applications. As reported previously, the rate of the heat transfer, $\dot{q}$, in a typical heat exchanger is given by the equation

$$\dot{q} = \dot{V} C_{PV} \Delta T \tag{1}$$

where $\dot{V}$ is the volumetric flux, ΔT the difference of temperature, and C_{PV} is known as isobaric volumetric specific heat, which is defined as the product of the density and isobaric specific heat, that is

$$C_{PV} = \rho C_P \tag{2}$$

The values of the isobaric volumetric specific heat were calculated and shown in Figure 4b. A similar trend to isobaric specific heat is observed, and an increase of up to 6.4% was found for the nanofluid with the highest concentration of Pd nanoparticles.

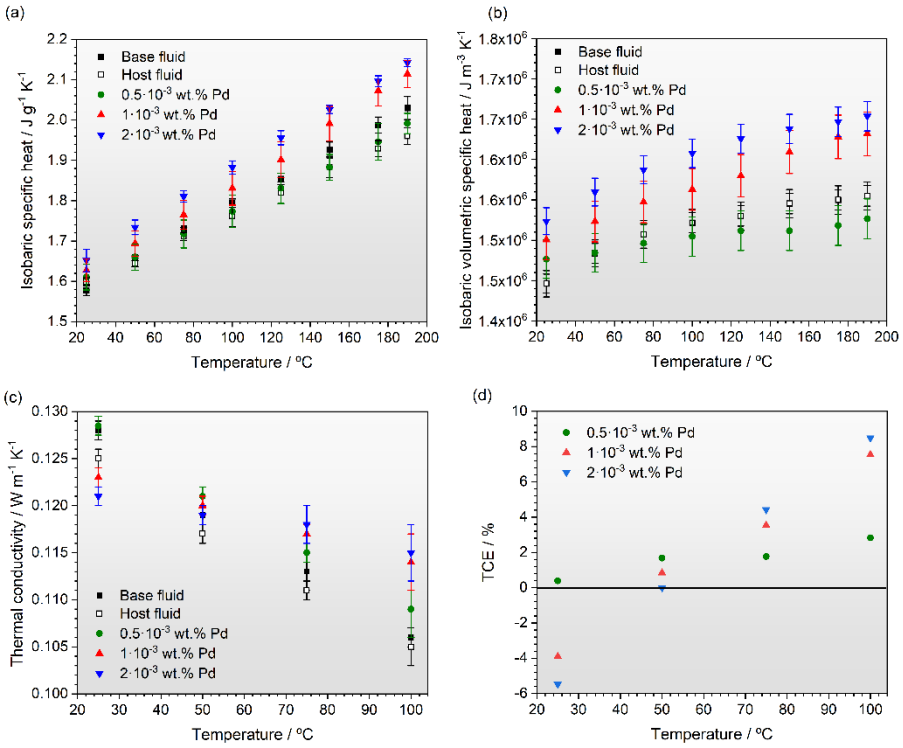

Figure 4. Isobaric specific heat (a), isobaric volumetric specific heat (b) and thermal conductivity values for the base fluid, the host fluid, the mixture of the base fluid and the surfactant, and the Pd-based nanofluids. Thermal conductivity enhancement (d) calculated for the nanofluids prepared.

Thermal conductivity is one of the most important properties in terms of the performance of heat transfer fluids. In this sense, the thermal conductivity of the Pd-based nanofluids was measured and compared with the values obtained for the base and host fluid. At 25 ºC, the value obtained for the base fluid was 0.128 W m^{-1} K^{-1}, in good agreement with the value of 0.126 W m^{-1} K^{-1} given by the supplier, a deviation of about 1.5%. In the whole range of temperatures under study, our values fit (by an average of 98.5%) the thermal conductivity values reported in the supplier datasheet [28]. Figure 4c shows the thermal conductivity values obtained. In all cases, a decrease is observed when the temperature increases. The effect of the addition of ODT as the surfactant can also be analysed from host fluid values

shown. A decrease of about 2% is observed in the temperature range under study. However, the addition of Pd nanoparticles leads to an increase in the thermal conductivity, mainly at higher temperatures. Figure 4d shows the values of the thermal conductivity enhancement, estimated as

$$TCE(\%) = 100 \cdot \left(k_{nf} - k_{bf}\right)/k_{bf} \quad (3)$$

where *k* is the thermal conductivity and the subscripts *bf* and *nf* refer to the base fluid and the nanofluids. The changes in thermal conductivity for the nanofluid with the lowest Pd concentration are very slight due to the small amount of Pd nanoparticles that remain after the stabilisation process, as discussed above. The behaviour for the other two nanofluids is different. At low temperatures, they show lower thermal conductivity values, while at higher temperatures the values obtained for the nanofluids are higher than for the base fluid, reaching an increase of about 8.5% for the most concentrated nanofluid, as is shown in Figure 4d. Previous studies using Pd and the eutectic mixture of diphenyl oxide and biphenyl have shown similar increase in thermal conductivity. Carrillo-Berdugo et al. reported increases about 11% [15].

3.3. Nanofluids performance

To analyse the performance of the nanofluids prepared in CSP-PTC technology, the outlet temperature (T_{out}) and the efficiency of the collector (Ψ_{coll}) was evaluated by using the models reported by Bellos et al. [34] and O'Keeffe et al [35]. In these models, 3D surface collectors under steady state conditions and turbulent flow are analysed. The equations, variables and

constants considered in both models are shown in greater depth in the Supporting Information.

To analyse the outlet temperature, the maximum temperature is defined by the nature of the heat transfer fluid used, that is the linear silicone-based fluid, which is 425 ºC according to the supplier. Bearing this in mind, the collector length needed to reach this maximum temperature was estimated considering several flow rates, in the range 100-300 L min^{-1}. This estimation was performed for the base fluid and the three nanofluids prepared. Figure 5 shows the values of the outlet temperature *vs* the collector length. As expected, the length needed to reach the maximum outlet temperature increases with the flow rate. In addition, for each flow rate value, the nanofluid with the lowest Pd nanoparticles concentration shows the lowest collector length to reach the maximum temperature, which means these nanofluids would lead to reduced costs because smaller CSP-PTCs installations could be developed. The decrease observed was about 4%. Considering that the typical flow rate in CSP-PTCs plants is about 150 L min^{-1}, the length for the base fluid is 229 m, and 220 m for the nanofluid with the lowest particle concentration. In the case of the nanofluids with a higher concentration, the collector needs to be longer, up to 241 and 244 m, for $1.0 \cdot 10^{-3}$ wt.% and $2.0 \cdot 10^{-3}$ wt.%, respectively. These are increases of about 5.2% and 6.5%, respectively.

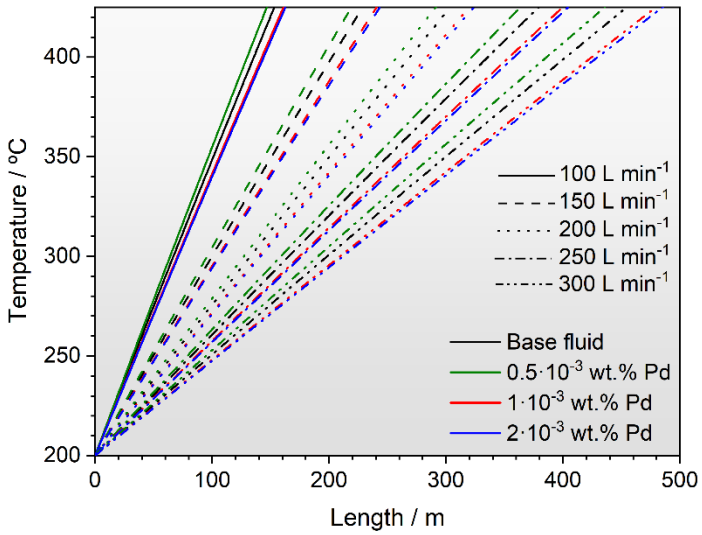

Figure 5. Outlet temperature (T_{out}) *vs* the collector length for the base fluid and the three nanofluids prepared considering flow rates in the range 100-300 L min^{-1}.

On the other hand, the overall system efficiency (ψ_{sys}) is obtained as

$$\Psi_{sys} = \Psi_{coll} \cdot \Psi_{hex} \quad (4)$$

where ψ_{coll} is the collector efficiency and ψ_{hex} is the heat exchanger efficiency. Thus, the collector efficiency was estimated according to Equations S2-S7 in the Supporting Information. Figure 6a shows the values obtained for the base fluid and the nanofluids for the same flow rate values. Slight changes in the collector efficiency are observed. An increase in the collector efficiency of about 1% is observed when the flow rate increases in the range studied, an insignificant increase. An increase of the collector efficiency is also observed for the nanofluids. For example, at 150 L min^{-1}, the collector efficiency for the base fluid is 0.727. The highest efficiency of 0.731 is found for the most concentrated nanofluid, an increase of 0.6%. Therefore, using the nanofluid in the PT collectors has a negligible effect. Thus, thermal conductivity and specific heat has an impact in the collector efficiency, as is

observed in the formula shown in the Supporting Information. But the increase reported for both properties (5.5% and 8.5% for isobaric specific heat and thermal conductivity) are not enough for leading to a significant enhance of the collector efficiency.

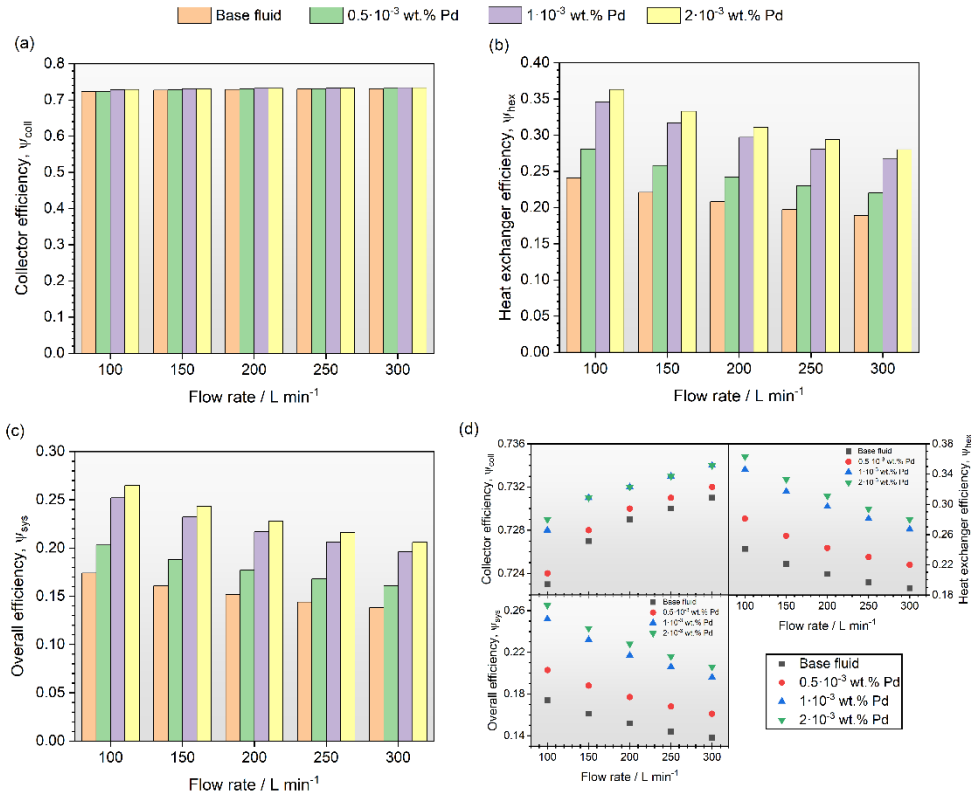

Figure 6. (a) PT collector efficiency, (b) heat exchanger efficiency, (c) overall system efficiency, (d) efficiencies in function of the heat transfer fluid considered.

The heat exchanger efficiency was estimated according to the number of transfer units (NTU) methodology [36]. Figures 6b and 6d show the values obtained. A decrease in the heat exchanger efficiency was observed when the flow rate increased. But the most important result is that the use of nanofluids increases the heat exchanger efficiency significantly. At a flow rate of 150 L min^{-1}, which used in CSP-PTC plants, the heat exchanger efficiency for

the base fluid is 0.221, and this value increases by about 16.7%, 43.4% and 50.7% for the nanofluids prepared, the higher Pd concentrations resulting in the greatest increases. These results show that the effect of the use of nanofluid is significant in the heat exchanger efficiency. According to the equations S8-S10 in the Supporting Information, an increase in the thermal conductivity leads to a significant enhancement in the heat exchanger efficiency, and the increase of the 8.5% in thermal conductivity is the main factor that produce sthe increase in the heat exchanger efficiency.

Next, the overall efficiency of the system was calculated. The results are shown in Figure 6c and 6d. We observe an increase in the overall efficiency for the nanofluids with respect to the base fluid. At a flow rate of 150 L min^{-1}, the efficiency increases from 0.161 for the base fluid to 0.243 for the most concentrated nanofluid ($2 \cdot 10^{-3}$ wt.%), an increase of 50.9%. As discussed above, this increase is mainly due to the improved heat exchanger efficiency resulting from the enhanced thermal properties of the nanofluids with respect to the base fluid, mainly from the increase in thermal conductivity. The increase in the overall efficiency found for the nanofluid with a concentration of 1.10^{-3} wt.% is 44.1%. This increase is lower than that obtained with the most concentrated nanofluid, but to decide between them we should consider the amount of nanoparticles used for each nanofluid and the fact that the nanofluid with the highest concentration needs a collector length of 244 m to reach the maximum outlet temperature, longer than the 241 m needed for the nanofluid with 1.10^{-3} wt.%. Thus, it will be necessary to determine the cost involved in both cases to decide which is the most promising nanofluid.

Finally, a comparison between the PDMS fluid, and the Pd-based nanofluids prepared in this work with respect to the conventional fluid used in CSP-PTC plants, that is the eutectic mixture of diphenyl oxide and biphenyl has been performed. The same simulation

methodology described previously has been used for estimate the ψ_{coll}, ψ_{hex} and ψ_{sys}. Table 1 shows the values calculated at a flow rate of 150 L min^{-1}, which is used in CSP-PTC plants. It is possible to observe that the conventional fluid shows higher collector end heat exchanger efficiency, which is mainly due to the higher heat capacity and thermal conductivity values, and lower dynamic viscosity. But this conventional fluid is not an environmentally friendly fluid, showing a certain degree of toxicity, and it is necessary to replace it. Thus, nanofluids based on PDMS can be a good option, but more research for enhancing their thermophysical properties are needed in the close future.

Table 1. ψ_{coll}, ψ_{hex} and ψ_{sys} values for the conventional fluid used in CSP-PTC plants and the base fluid and the $2.0 \cdot 10^{-3}$ wt.% Pd nanofluid, estimated at a flow rate of 150 L min^{-1}.

	DPO-BP	**PDMS**	**$2.0 \cdot 10^{-3}$ wt.% Pd**
ψ_{coll}	0.741	0.727	0.731
ψ_{hex}	0.466	0.221	0.333
ψ_{sys}	0.345	0.161	0.243

3.4. Interactions at Pd-PDMS interfaces and implications

Exploring the chemistry of solid-liquid interfaces and their correlation with the efficiency of energy storage and transfer in nanofluids is currently recognised as a frontier topic in this area of knowledge because the performance of nanofluids in heat transfer applications will depend on these properties. By understanding how the nature of the chemical interactions between species at the solid-liquid interface affects the overall specific heat or thermal conductivity of these colloids, we can rationalise the choice of a nanomaterial to improve the thermal properties of the preferred HTF for a given application. Whilst studying a single system does not significantly build up a solid perspective on the matter, as we are starting to

study this new PDMS-based fluid for CSP plants, it is important to benchmark the interfacial physical and chemical descriptors and the effective thermal properties of as many solid-liquid pairs as possible for such a purpose.

The methodology detailed that we systematically probed the interactions of HMDS with Pd (111), (100) and (110) surfaces by considering a variety of initial configurations in which Si atoms of HMDS are located at one of the high symmetry sites on these surface terminations. Figure 7 identifies the relevant sites on its left-hand side, and displays the well-converged, non-redundant adsorption structures for HMDS at Pd surfaces on its right-hand side. The energy accompanying each adsorption structure was calculated at the same level of theory by taking the free energy of the supercell and subtracting the free energies of the surface termination and the gas phase molecule, all of which are relaxed separately. Adsorption is, in all cases, an exothermic process. The order of magnitude of the adsorption energy values predicted by DFT indicates that no chemical interactions beyond van der Waals forces are controlling the adsorption process. The relative stability of the different adsorption geometries merely results from the favoured occupancy of sites where van der Waals forces are maximised, with no outstanding differences as there is no chemical bonding. Overall, adsorption energy values are also higher in magnitude than the bulk cohesive energy (*i.e.*, *ca.* -0.5 eV per molecule using the level of theory at hand) and thermal vibrations (*i.e.*, *ca.* 90 meV per molecule at 425 ºC, which is the maximum operating temperature for this fluid). Therefore, it is safe to conclude that a significant driving force exists for the adsorption of HMDS on Pd surfaces.

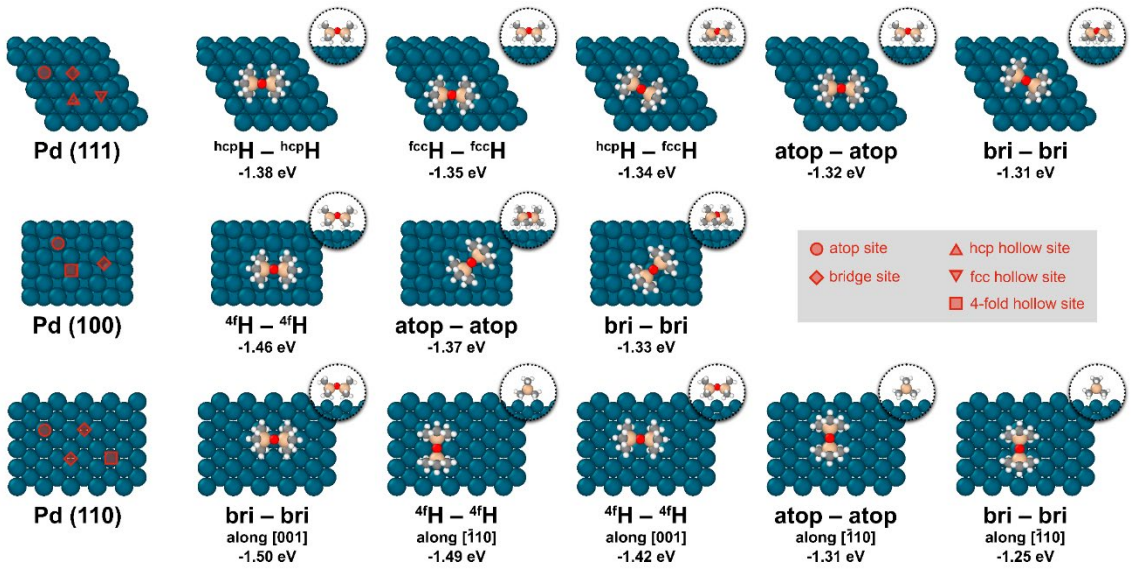

Figure 7. Geometries and adsorption energies for the HMDS molecule on Pd (111), (100) and (110) surfaces. Geometries are labelled according to the high-symmetry sites occupied by Si atoms as HMDS is relaxed on each surface termination. Visualisations were made with OVITO [37].

In previous studies by our group [14, 38], we have thoroughly studied the interface between Pd surfaces and the eutectic and azeotropic mixture of diphenyl oxide (DPO) and biphenyl (BP), which has been the HTF of choice for CSP plants until now. This paper represents an excellent opportunity to compare Pd-PMDS and Pd-DPO/BP nanofluids in terms of their interface chemistry and, for instance, their specific heat. Pd-DPO/BP interfaces are distinguished by the adsorption of the phenyl rings via chemical bonding onto Pd surfaces, which is possible by the donation of electrons from the highest occupied π molecular orbital of the phenyl rings to the d-band of Pd and back-donation from the d-band to the lowest unoccupied π* molecular orbital. Pd-HMDS interfaces, as described above, are governed by van der Waals forces only. Consequently, the adsorption energies of between 3.5-4.5 eV of Pd-DPO/BP [14] are much higher than those of Pd-HMDS, which fall within the range of

1.2-1.5 eV. These datasets are directly comparable, as they were both produced at the same level of theory.

One of our studies [38] conducted a series of classical molecular dynamics simulations using different interatomic potentials to represent the interactions at the interface between a Pd nanoparticle and a bulk of DPO/BP molecules. The key finding from this research underscores that the stronger the interactions (represented by the interatomic potential under consideration) at interfaces, the greater the specific heat enhancement. Based on this general observation, it can be anticipated that enhancements in specific heat with respect to the base fluid are higher in Pd-DPO/BP nanofluids than in Pd-PDMS nanofluids. In fact, experimental data suggests so. There are substantial variations in the achievable enhancements in specific heat (and other physical properties) when using the same nanomaterial in different fluids due to the different chemistry of their interfaces. It is difficult of model to make a side-by-side comparison between these systems, as the only well stablished predictive model that exist for the specific of nanofluids deals with them as ideal mixtures of non-interacting components and includes no information about the contribution of interfaces to this macroscopic property. There is an incipient modelling attempt by Leonardi et al. [39] that considers this contribution. We are, unfortunately, at early stages of research on the matter, but we will try to continue developing a theoretical framework to correlate the strength of chemical interactions at interfaces with the specific heat enhancements in nanofluids.

4. Conclusions

Three nanofluids based on a linear silicone-based fluid and with different concentrations of Pd nanoparticles have been prepared and widely characterized. Their physical stability was analysed, all three showing an aggregation period for several days after preparation until they

reached stability. The properties of interest of the nanofluids for CSP-PTC plants were measured and analysed, namely surface tension, density, viscosity, isobaric specific heat and thermal conductivity. No significant changes were found in the surface tension with respect to the base fluid, while their density increased by up to 0.65%. In addition, the base fluid showed Newtonian behaviour, as did the three nanofluids prepared. The highest increase in viscosity, about 2.5%, was observed for the most concentrated nanofluid. This is an interesting result, because the presence of Pd nanoparticles in our nanofluids does not lead to a significant increase in the viscosity values, and they also maintain the Newtonian behaviour of the base fluid. Therefore, the use of these nanofluids does not produce a significant increase in the pumping power needed, the friction factor or pressure drops. Thermal properties were measured. The isobaric specific heat of the nanofluids increased with respect to the base fluid, the highest increase being about 5.5%. Increases in thermal conductivity were also found. At higher temperatures, the values obtained for the nanofluids were higher than for the base fluid, reaching an increase of about 8.5% for the most concentrated nanofluid.

Finally, DFT simulations showed that the adsorption on Pd surfaces is weak, only van der Waals forces mediating in this case. The interface chemistry that arises between this metal and each fluid justifies the differences observed in specific heat enhancement with respect to the base fluid. These differences underscore the necessity for a theoretical framework that allows us to determine in advance the best nanomaterials to improve the thermal properties of a preferred HTF for any given application.

From the values of these properties, the efficiency of the nanofluids in CSP-PTC plants was modelled and a significant increase of about 50% was found, which is a promising result. This result shows significant implications for this technology, in order to extend the use of

CSP-PTC plants for producing electricity to meet the enormous demand for energy while creating the lowest environmental impact, which is one of the main challenges of our society. In this sense, our results are promising, but more research are needed in order to increase the load of heat carriers in this base fluid for improving the enhancement of the thermal properties which are the driving force for reaching the highest possible efficiency of CSP-PTC plants.

Supporting Information

I. Calculation of the outlet temperature and the collector efficiency for surface parabolic trough collectors (PTCs). II. Calculation of the heat exchanger effectiveness for surface and volumetric PTCs.

Acknowledgements

P. Estellé was Visiting Researcher at University of Cádiz during the first semester 2023. He gratefully acknowledges J. Navas and his group for their warm welcome during this period, and the support of the National Council of Universities (CNU) and University of Rennes. Also, this work was supported by the *Ministerio de Ciencia e Innovación del Gobierno de España* [grant numbers TED2021-132518B-I00, UNCA15-CE-2945]; the *Ministerio de Universidades del Gobierno de España* for the allocated budget from the NextGenerationEU programme to public universities for the requalification of the Spanish university system, which funds his postdoctoral position at the University of Cadiz in the form of a *Margarita*

Salas fellowship [grant number 2021-067/PN/MS-RECUAL/CD]; the University of Cadiz's high performance computing service for research.

References

[1] R. Gomez-Villarejo, E.I. Martin, J. Navas, A. Sanchez-Coronilla, T. Aguilar, J.J. Gallardo, R. Alcantara, D. De los Santos, I. Carrillo-Berdugo, C. Fernandez-Lorenzo, Ag-based nanofluidic system to enhance heat transfer fluids for concentrating solar power: Nano-level insights, Appl Energ 194 (2017) 19-29. https://doi.org/10.1016/j.apenergy.2017.03.003

[2] J. Khan, M.H. Arsalan, Solar power technologies for sustainable electricity generation - A review, Renew Sust Energ Rev 55 (2016) 414-425. https://doi.org/10.1016/j.rser.2015.10.135

[3] U. Desideri, F. Zepparelli, V. Morettini, E. Garroni, Comparative analysis of concentrating solar power and photovoltaic technologies: Technical and environmental evaluations, Appl Energ 102 (2013) 765-784. https://doi.org/10.1016/j.apenergy.2012.08.033

[4] D.R. Rajendran, E.G. Sundaram, P. Jawahar, V. Sivakumar, O. Mahian, E. Bellos, Review on influencing parameters in the performance of concentrated solar power collector based on materials, heat transfer fluids and design, J Therm Anal Calorim 140 (2020) 33-51. https://doi.org/10.1007/s10973-019-08759-8

[5] X. Jin, H.Q. Guan, R.J. Wang, L.Z. Huang, C. Shao, The most crucial factor on the thermal conductivity of metal-water nanofluids: Match degree of the phonon density of state, Powder Technol 412 (2022) https://doi.org/10.1016/j.powtec.2022.117969

[6] A. Karakas, S. Harikrishnan, H.F. Oztop, Preparation of EG/water mixture-based nanofluids using metal-oxide nanocomposite and measurement of their thermophysical properties, Therm Sci Eng Prog 36 (2022) https://doi.org/10.1016/j.tsep.2022.101538

[7] A. Banisharif, P. Estellé, A. Rashidi, S. Van Vaerenbergh, M. Aghajani, Heat transfer properties of metal, metal oxides, and carbon water-based nanofluids in the ethanol condensation process, Colloid Surface A 622 (2021) https://doi.org/10.1016/j.colsurfa.2021.126720

[8] L.S. Sundar, F. Shaik, Laminar convective heat transfer, entropy generation, and exergy efficiency studies on ethylene glycol based nanofluid containing nanodiamond nanoparticles, Diam Relat Mater 131 (2023) 109599. https://doi.org/10.1016/j.diamond.2022.109599

[9] I. Carrillo-Berdugo, P. Estellé, E. Sani, L. Mercatelli, R. Grau-Crespo, D. Zorrilla, J. Navas, Optical and Transport Properties of Metal-Oil Nanofluids for Thermal Solar Industry: Experimental Characterization, Performance Assessment, and Molecular Dynamics Insights, Acs Sustain Chem Eng 9 (2021) 4194-4205. https://doi.org/10.1021/acssuschemeng.1c00053

[10] D.M. De los Santos, I. Carrillo-Berdugo, A. Dominguez-Nunez, J.A. Poce-Fatou, D. Zorrilla, J. Navas, NiO nanowire-containing heat transfer nanofluids for CSP plants: Experiments and simulations to promote their application, J Mol Liq 361 (2022) https://doi.org/10.1016/j.molliq.2022.119593

[11] J. Navas, P. Martinez-Merino, A. Sanchez-Coronilla, J.J. Gallardo, R. Alcantara, E.I. Martin, J.C. Pinero, J.R. Leon, T. Aguilar, J.H. Toledo, C. Fernandez-Lorenzo, MoS2 nanosheets vs. nanowires: preparation and a theoretical study of highly stable and efficient

nanofluids for concentrating solar power, J Mater Chem A 6 (2018) 14919-14929. https://doi.org/10.1039/c8ta03817a

[12] M.H. Wan, B. Xu, L. Shi, N.B. Zheng, Z.Q. Sun, The dynamic stability of silicone oil-based MWCNT nanofluids under high-temperature, high-flux irradiation, and shear-flow conditions, Powder Technol 424 (2023) 118508. https://doi.org/10.1016/j.powtec.2023.118508

[13] N. Aslfattahi, L. Samylingam, A.S. Abdelrazik, A. Arifutzzaman, R. Saidur, MXene based new class of silicone oil nanofluids for the performance improvement of concentrated photovoltaic thermal collector, Sol Energ Mat Sol C 211 (2020) 110526. https://www.doi.org/10.1016/j.solmat.2020.110526

[14] I. Carrillo-Berdugo, S.D. Midgley, R. Grau-Crespo, D. Zorrilla, J. Navas, Understanding the Specific Heat Enhancement in Metal-Containing Nanofluids for Thermal Energy Storage: Experimental and Ab Initio Evidence for a Strong Interfacial Layering Effect, Acs Appl Energ Mater 3 (2020) 9246-9256. https://www.doi.org/10.1021/acsaem.0c01556

[15] I. Carrillo-Berdugo, J. Sampalo-Guzmán, A. Domínguez-Núñez, T. Aguilar, P. Martínez-Merino, J. Navas, Are Nanofluids Suitable for Volumetric Absorption in PTC-CSP Plants? An Exemplified, Realistic Assessment with Characterized Metal-Oil Nanofluids, Energ Fuel 36 (2022) 8413-8421. 10.1021/acs.energyfuels.2c01759

[16] G. Kresse, J. Furthmuller, Efficiency of ab-initio total energy calculations for metals and semiconductors using a plane-wave basis set, Comp Mater Sci 6 (1996) 15-50. http://www.doi.org/10.1016/0927-0256(96)00008-0

[17] G. Kresse, J. Furthmuller, Efficient iterative schemes for ab initio total-energy calculations using a plane-wave basis set, Phys Rev B 54 (1996) 11169-11186. https://www.doi.org/10.1103/PhysRevB.54.11169

[18] G. Kresse, J. Hafner, Ab-Initio Molecular-Dynamics Simulation of the Liquid-Metal Amorphous-Semiconductor Transition in Germanium, Phys Rev B 49 (1994) 14251-14269. https://www.doi.org/10.1103/PhysRevB.49.14251

[19] Kresse, G.; Vogtenhuber, D.; Marsman, M.; Kaltak, M.; Karsai, F.; Schlipf, M. Vienna Ab-initio Simulation Package (VASP), 6.3.1; 2022,

[20] J.P. Perdew, K. Burke, M. Ernzerhof, Generalized gradient approximation made simple, Phys Rev Lett 77 (1996) 3865-3868. https://www.doi.org/10.1103/PhysRevLett.77.3865

[21] S. Grimme, J. Antony, S. Ehrlich, H. Krieg, A consistent and accurate ab initio parametrization of density functional dispersion correction (DFT-D) for the 94 elements H-Pu, J Chem Phys 132 (2010) 154104. https://www.doi.org/10.1063/1.3382344

[22] S. Grimme, S. Ehrlich, L. Goerigk, Effect of the Damping Function in Dispersion Corrected Density Functional Theory, J Comput Chem 32 (2011) 1456-1465. https://www.doi.org/10.1002/jcc.21759

[23] G. Kresse, J. Hafner, Norm-Conserving and Ultrasoft Pseudopotentials for First-Row and Transition-Elements, J Phys-Condens Mat 6 (1994) 8245-8257. https://www.doi.org/10.1088/0953-8984/6/40/015

[24] G. Kresse, D. Joubert, From ultrasoft pseudopotentials to the projector augmented-wave method, Phys Rev B 59 (1999) 1758-1775. DOI 10.1103/PhysRevB.59.1758

[25] H.J. Monkhorst, J.D. Pack, Special Points for Brillouin-Zone Integrations, Phys Rev B 13 (1976) 5188-5192. https://www.doi.org/10.1103/PhysRevB.13.5188

[26] J.D. Pack, H.J. Monkhorst, Special Points for Brillouin-Zone Integrations - Reply, Phys Rev B 16 (1977) 1748-1749. DOI 10.1103/PhysRevB.16.1748

[27] M. Methfessel, A.T. Paxton, High-Precision Sampling for Brillouin-Zone Integration in Metals, Phys Rev B 40 (1989) 3616-3621. https://www.doi.org/10.1103/PhysRevB.40.3616

[28] https://www.wacker.com/h/en-us/medias/HELISOL-5A-en-2023.03.22.pdf. (accessed 2023-09-20)

[29] D. Cabaleiro, C. Gracia-Fernández, J.L. Legido, L. Lugo, Specific heat of metal oxide nanofluids at high concentrations for heat transfer, Int J Heat Mass Tran 88 (2015) 872-879. https://www.doi.org/10.1016/j.ijheatmasstransfer.2015.04.107

[30] N.S.S. Mousavi, S. Kumar, Effective heat capacity of ferrofluids - Analytical approach, Int J Therm Sci 84 (2014) 267-274. https://www.doi.org/10.1016/j.ijthermalsci.2014.05.012

[31] D. Shin, D. Banerjee, Enhancement of specific heat capacity of high-temperature silica-nanofluids synthesized in alkali chloride salt eutectics for solar thermal-energy storage applications, Int J Heat Mass Tran 54 (2011) 1064-1070. https://www.doi.org/10.1016/j.ijheatmasstransfer.2010.11.017

[32] D. Shin, D. Banerjee, Enhanced Specific Heat Capacity of Nanomaterials Synthesized by Dispersing Silica Nanoparticles in Eutectic Mixtures, J Heat Trans-T Asme 135 (2013) 032801. https://www.doi.org/10.1115/1.4005163

[33] D. Shin, D. Banerjee, Specific heat of nanofluids synthesized by dispersing alumina nanoparticles in alkali salt eutectic, Int J Heat Mass Tran 74 (2014) 210-214. https://www.doi.org/10.1016/j.ijheatmasstransfer.2014.02.066

[34] E. Bellos, C. Tzivanidis, Analytical expression of parabolic trough solar collector performance, Designs 2 (2018) 9. https://www.doi.org/103390/designs2010009

[35] G.J. O'Keeffe, S.L. Mitchell, T.G. Myers, V. Cregan, Modelling the efficiency of a nanofluid-based direct absorption parabolic trough solar collector, Sol Energy 159 (2018) 44-54. https://doi.org/10.1016/j.solener.2017.10.066

[36] T.L. Bergman, A.S. Lavine, F.P. Incropera, D.P. Dewitt, Fundamentals of Heat and Mass Transfer. 7th Ed. edn. John Wiley & Sons, New Jersey, USA, 2011.

[37] A. Stukowski, Visualization and analysis of atomistic simulation data with OVITO-the Open Visualization Tool, Model Simul Mater Sc 18 (2010) 015012. https://www.doi.org/10.1088/0965-0393/18/1/015012

[38] I. Carrillo-Berdugo, R. Grau-Crespo, D. Zorrilla, J. Navas, Interfacial molecular layering enhances specific heat of nanofluids: Evidence from molecular dynamics, J Mol Liq 325 (2021) 115217. https://www.doi.org/10.1016/j.molliq.2020.115217

[39] E. Leonardi, A. Floris, S. Bose, B. D'Aguanno, Unified Description of the Specific Heat of Ionic Bulk Materials Containing Nanoparticles, Acs Nano 15 (2021) 563-574. https://www.doi.org/10.1021/acsnano.0c05892

Table of Content

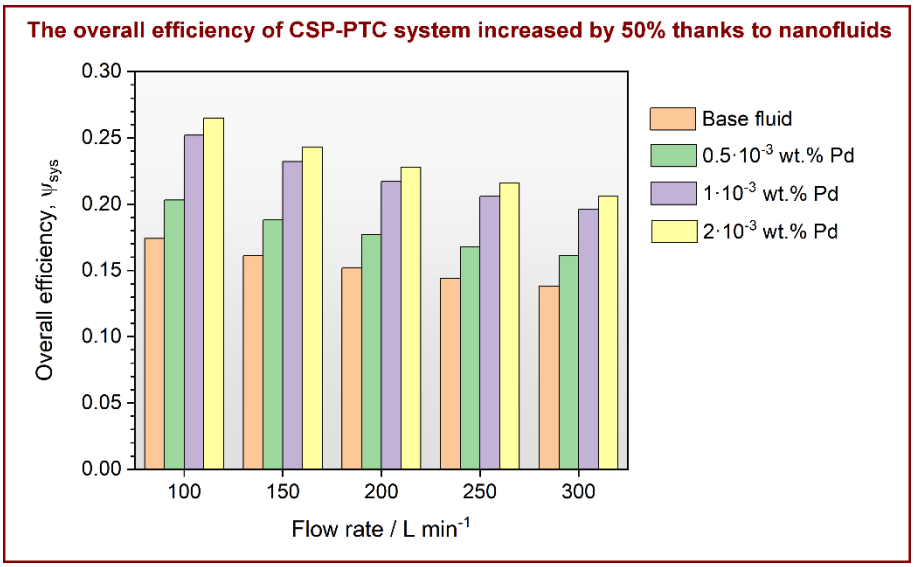

Synopsis

Pd nanoparticles and a linear silicone-based fluid were used for preparing highly efficient nanofluids for being applied in CSP-PTC technology.